Influence of Chemical Structure and Solubility of Bisamide Additives on the Nucleation of Isotactic Polypropylene and the Improvement of Its Charge Storage Properties†

Nils Mohmeyer,‡,|| Hans-Werner Schmidt,*,‡ Per Magnus Kristiansen,§ and Volker Altstädt⊥

Macromolecular Chemistry I, Bayreuther Institut für Makromolekülforschung (BIMF) and Bayreuther Zentrum für Grenzflächen und Kolloide (BZKG), University Bayreuth, D-95447 Bayreuth, Germany, Ciba Specialty Chemicals, CH-4002 Basel, Switzerland, and Polymer Engineering, University Bayreuth, D-95447 Bayreuth, Germany

Received February 15, 2006; Revised Manuscript Received May 3, 2006

ABSTRACT: A comparative study on the influence of chemical structure and solubility of a series of low-molecular-weight 1,4-phenylene−bisamides in isotactic polypropylene (*i*-PP) was conducted to explore their performance as nucleating agents and electret additives. The series consists of three isomers of dicyclohexyl-substituted 1,4-phenylene−bisamide and three asymmetrically substituted cyclohexyl/*n*-alkyl-1,4-phenylene−bisamides with different chain lengths. The symmetry of the molecules, the type of substitution and the length of the alkyl chain influence the solubility in the *i*-PP melt, the nucleation efficiency, the ratio of the α- to *β*-crystal modification and the charge storage properties. The best *β*-nucleating efficiency was observed for the symmetrically substituted compounds, whereas the nucleation efficiency was substantially reduced in the presence of *n*-alkyl-substituents. The charge storage behavior of *i*-PP was improved only for the three dicyclohexyl-substituted 1,4-phenylene bisamides at concentrations of 100 ppm and even below. For example, a film comprising 10 ppm additive displayed charge retention of 90% after an accelerated aging (annealing for 24 h at 90 °C).

1. Introduction

Polymers are increasingly being applied as dielectrics and electret materials.[1] Generally, polymeric electret materials are based on perfluorinated polymers such as polytetrafluorethylene (PTFE) due to their outstanding charge storage properties.[2] However, with respect to the poor processability, high price and recyclability, it would be interesting to substitute perfluorinated polymers by a commodity polymer such as isotactic polypropylene (*i*-PP). Improvements of the charge storage behavior of i-PP have been achieved by modification of the stereochemical composition of the polymer,[3] by increasing the crystallinity[4] and through mechanical deformation.[5] Recently, it was found that nucleating agents can be advantageously applied to improve the charge storage properties of i-PP either by the formation of elongated voids via particles during a deformation process[6] or by introducing charge traps by adding minor amounts of triphenylamine-based additives.[7]

Nucleating agents are applied to raise the crystallization temperature of *i*-PP which translates into reduced processing cycle times and, in addition, leads to improved mechanical and optical properties.[8,9] Besides the well-known sorbitol-based nucleating and clarifying agent[10−14] (e.g., 1,3:2,4-bis(dimethylbenzylidene)-D-sorbitol (DMDBS)), recently the class of substituted benzene-1,3,5-trisamides was found to provide highly efficient nucleating agents and in some cases even clarifiers for *i*-PP.[15] Depending on the concentration and processing temperature these additives may or may not be soluble in the *i*-PP melt. The soluble fraction of the additive self-assembles/crystallizes upon cooling from the melt into fine fibrillar supramolecular nanostructures with a large surface area on which the i-PP nucleates. In contrast, other nucleating agents such as sodium 2,2′-methylene-bis(4,6-di-*tert*-butylphenyl) phosphate (NA11) are salts which are virtually insoluble in the *i*-PP melt. The latter phosphate salt favors the formation of the α-crystal modification.[16,17] The nucleating agent *N*,*N*′-dicyclohexyl-2,6-naphthalenedicarboxamide (NU100) promotes the *β*-crystal modification of i-PP.[18−23] NU100 was found to be partially soluble in the *i*-PP melt and is inefficient in the concentration range below 300 ppm.[18] Both nucleating agents, NA11 and NU100, have been employed in order to investigate the influence of the α and *β*-crystal modification on the charge storage properties.[6] Neither the phosphate salt nor the bisamide improves the electret properties of compact films at the investigated concentrations of 0.05−0.3 wt %. However, by utilizing the dispersed insoluble particles of the phosphate salt, voids can be formed during biaxial stretching. The undissolved particles act as stress concentrators, leading to the formation of elongated microvoids in the film. In the resulting porous *i*-PP films, these cavities provide effective barriers for the charge drift whereby the electret properties are substantially improved.[6] In contrast to the generation of porous films, an alternative way to improve the electret properties of compact *i*-PP films is the use of charge trapping agents. It could be shown that triphenylamine trisamide derivatives, which are completely soluble at the effective concentration, self-assemble upon cooling into isolated nanoaggregates, acting as charge traps in the *i*-PP film, thus improving the electret properties.[7] However, the magnitude of improvement of the charge storage properties was not sufficient.

† Dedicated to Prof. Gerhard M. Sessler on the occasion of his 75th birthday.

* Corresponding author. E-mail: hans-werner.schmidt@uni-bayreuth.de. Telephone: +(49) 921/55-3200. Fax: +(49) 921/55-3206.

‡ Macromolecular Chemistry I, Bayreuther Institut für Makromolekülforschung (BIMF) and Bayreuther Zentrum für Grenzflächen und Kolloide (BZKG), University Bayreuth.

§ Ciba Specialty Chemicals.

⊥ Polymer Engineering, University Bayreuth.

|| E-mail: nils.mohmeyer@uni-bayreuth.de.

10.1021/ma060340q CCC: $33.50
Published on Web 07/20/2006

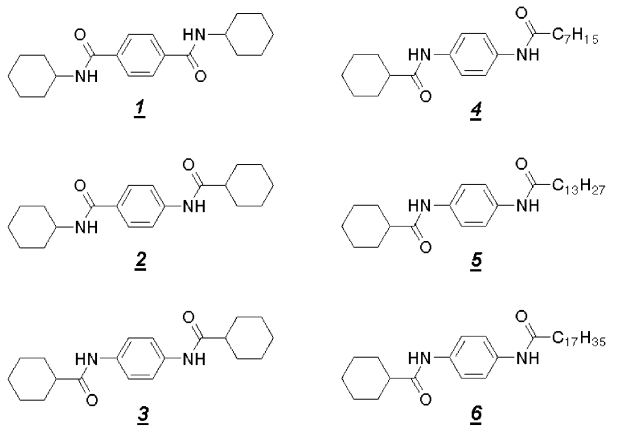

Figure 1. Chemical structures of the investigated additives: isomers of dicyclohexyl-substituted 1,4-phenylene bisamides **1**−**3** and cyclohexyl/*n*-alkyl-substituted 1,4-phenylene bisamides with a variation of the length of the alkyl chain **4**−**6**.

The aim of this paper is to systematically study the influence of a series of 1,4-phenylene−bisamides on the nucleation efficiency and electret properties of *i*-PP. Three isomers of dicyclohexyl-substituted 1,4-phenylene−bisamides **1**−**3** and three asymmetrically substituted cyclohexyl/*n*-alkyl-1,4-phenylene−bisamides **4**−**6** with different chain lengths were investigated (Figure 1). The effect of these structural variations on the nucleation efficiency, on the type of crystal modification, and on the charge storage properties will be discussed. The additives are studied in a concentration range from as low as 0.0005 wt % (5 ppm) up to 0.25 wt % (2500 ppm).

2. Experimental Section

Materials. Isotactic polypropylene was obtained as reactor powder from Borealis (Linz, Austria) and extracted with acetone, ethanol, and cyclohexane, each for 2 days in order to remove all stabilizers and other additives. Solvents for synthesis were purified and dried when necessary according to standard procedures. The amines and acid chlorides employed for synthesis were obtained from Aldrich and used as received. The dicyclohexyl-substituted 1,4-phenylene bisamides **1**−**3** were synthesized according to procedures described elsewhere.[21,24] The synthesis of cyclohexyl/*n*-alkyl-substituted 1,4-phenylenediamine derivatives **4**−**6** is described in our previous work.[25]

Sample Preparation. Polymer/additive mixtures were prepared in a laboratory-scale, co-rotating mini-twin-screw extruder (Technical University Eindhoven, The Netherlands) at 240 °C under nitrogen for 4 min. The extruded mixtures were subsequently melted at 260 °C under nitrogen for 2 min and injection molded using a microinjector (DACA Instruments, Goleta, CA) into specimens of 1.1 mm thickness and 25 mm diameter. Films of about 50 μm thickness were prepared from the injection-molded specimen by compression molding in a metal frame between cleaned Kapton foils and metal plates by melting at 260 °C for 3 min and pressing for 4 min at 15 kN in a laboratory press (P. O. Weber), followed by cooling at an average cooling rate of 10 K/min to room temperature between the hot metal plates.

Thermal Properties. The melting temperature and weight loss of the bisamides were determined by a coupled dynamic thermogravimetric analysis (TGA) and differential thermal analysis (DTA) instrument, Netzsch STA 409. The crystallization temperature of *i*-PP/additive mixtures was determined by differential scanning calorimetry (DSC Diamond, Perkin-Elmer). Measurements were performed with i-PP/additive mixtures of 8−10 mg at a standard heating and cooling rate of 10 °C/min under nitrogen starting from 130 to 230 °C, samples were subsequently held at 230 °C for 5 min to ensure complete melting of the polymer, followed by cooling to 50 °C. Reported values for the crystallization temperature (T_c) refer to the peak temperatures in the respective thermograms.

Optical Properties. The standard optical characteristic "haze" was measured on injection-molded plaques (1.1 mm thickness) with a "Haze-Gard Plus" instrument (BYK Gardner GmbH, Germany), according to ASTM D-1003.[26]

Optical Microscopy. Optical micrographs were taken between crossed polarizers using a Nikon microscope equipped with a hot-stage (Mettler Toledo FP82HT) at a standard scan rate of 5 °C·min^{-1}. The additive dissolution and recrystallization temperatures were determined by polarized light microscopy as described by Kristiansen et al. in ref 14. In heating experiments at a scan rate of 5 °C·min^{-1}, the dissolution temperatures ($T_{d,a}$) were taken to be that temperature where the last crystal of the additive disappeared completely. Upon cooling, additive crystallization temperatures ($T_{c,a}$) were taken where the first birefringent crystal appeared.

***β*-Content.** Wide-angle X-ray scattering (WAXS) patterns were recorded in transmission with a Bruker D8 Advance X-ray diffractometer. The wavelength used was Cu Kα ($\lambda = 1.54$ Å) and spectra were recorded in the 2θ range of 8−30° (step size 0.025°). The content of the β-crystal modification was determined according to standard procedures described in the literature,[27] employing the relation

$$k = \frac{H_\beta(300)}{H_\beta(300) + H_\alpha(110) + H_\alpha(040) + H_\alpha(130)} \qquad (1)$$

where $H_{\Omega(hkl)}$ denotes the intensity of the respective (*hkl*) peak belonging to phase Ω (α or β; always with respect to the amorphous halo).

Charge−Storage Properties. Films of 4 cm × 5 cm area and about 50 μm thickness of the different polypropylene/additive mixtures were glued onto aluminum plates with conductive double-side adhesive tape. All samples were charged for 30 s using a point-to-plate corona setup with a grid for limitation of the surface potential. Corona voltages of +12.5 kV and grid voltages of +400 V were employed. The surface potential of each sample was measured at five defined positions with an electrostatic voltmeter (244 A, Monroe). Measurements were performed directly after charging at room temperature and after annealing at 90 °C for cumulative periods of 30, 90, 180, 360, 720, and 1440 min. The potential measurements were performed at room temperature, outside the heating chamber. Thus, the samples were also subjected to several heating and cooling cycles during the isothermal charge decay measurements.

3. Results and Discussion

3.1. Synthesis, Thermal, and Solubility Properties. The symmetric bisamide isomers **1** and **3** were synthesized in a one-step condensation reaction. In the case of *N*,*N*′-dicyclohexyl-terephthalamide **1**, terephthalic acid chloride was reacted with an excess of cyclohexylamine in *N*-methyl-2-pyrrolidone (NMP) in the presence of triethylamine as base as described in the literature.[21,24] Isomer **3** was synthesized from *p*-phenylenediamine and cyclohexanecarboxylic acid chloride under the same conditions. The asymmetrical isomer cyclohexanecarboxylic acid−(4-cyclohexoylaminophenyl)amide (**2**) with a differing orientation of the amide groups was obtained in three steps. In the first step, 4-nitrobenzoic acid chloride was reacted with cyclohexylamine. The resulting nitro compound was reduced with hydrogen and palladium on activated carbon as catalyst to the corresponding amine and further converted with the cyclohexanecarboxylic acid chloride to compound **2**. The compounds were recrystallized from *N*,*N*′-dimethylformamide (DMF). The melting temperatures (T_m) were determined by differential scanning calorimetry (DSC) and are listed in Table 1. The

Table 1. Additive Melting (T_m), Dissolution ($T_{d,a}$), and Recrystallization Temperatures ($T_{c,a}$) of the Investigated Bisamide Derivatives 1−6 at a Concentration of 0.25 wt % in *i*-PP

compound	T_m [°C]	$T_{d,a}$ [°C]	$T_{c,a}$ [°C]
1	329[a]	256	212
2	280[a]	215	182
3	285[a]	244	210
4	225	182	165
5	215	<170[b]	153
6	211	<170[b]	147

[a] Melting with simultaneous evaporation. [b] No birefringent structures could be observed at 170 °C directly after the melting of *i*-PP.

highest melting temperature of 329 °C was found for compound **1** based on terephthalic acid. The inversion of the amide groups in compound **3** resulted in a significantly lower melting temperature of 285 °C. As expected, the asymmetric compound **2** had the lowest melting temperature of this series (280 °C). As previously demonstrated for the trisamide/polypropylene system,[15] additive dissolution temperatures can be determined by polarized light microscopy. In heating experiments at a scan rate of 5 °C/min, the dissolution temperatures ($T_{d,a}$) were taken to be that temperature where the last crystals disappeared completely. The crystallization temperatures ($T_{c,a}$) of the additives were taken to be that temperature where the first crystals appeared upon cooling. Table 1 summarizes the determined dissolution and crystallization temperatures of the different additives in *i*-PP at a concentration of 0.25 wt %. It is interesting to note that the symmetric isomers **1** and **3** displayed very similar dissolution behavior ($T_{d,a}$ of 256 °C for **1** and 244 °C for **3**), whereas the asymmetrical isomer **2** more readily dissolved ($T_{d,a}$ = 215 °C). Subsequently, the samples were cooled at a rate of 5 °C/min and the dendtritic additive structures evolved from the melt. The crystallization temperatures of the additives are 33−44 °C lower than the dissolution temperatures. Compound **1** and **3** crystallize at a similar temperatures and compound **2** has the lowest crystallization temperature at 182 °C. During the crystallization process, the additives form three-dimensional fibrillar dendritic structures in the *i*-PP melt, which can be visualized in optical light microscopy between crossed polarizers (Figure 2). In these experiments the samples were heated to 260 °C, at which point all additives were found to be completely soluble in the polymer melt. It is interesting to note that the asymmetrical compound **2** forms twisted fibrillar aggregates, as can be seen in Figure 2. The different orientation of the molecules within one fibril with respect to the orientation of the crossed polarizers results in a periodic extinction of the birefringence, a feature not visible in the dendritic fibrillar structures formed by additives **1** and **3**.

The three asymmetrically substituted cyclohexyl/*n*-alkyl-1,4-phenylene−bisamides **4**−**6**, which exhibit the same orientation of the amide groups as compound **3**, were synthesized in three steps.[25] First, 4-nitroaniline and cyclohexanecarboxylic acid chloride were reacted and the resulting nitro compound was reduced with hydrogen and palladium on activated carbon to the corresponding amine. In the final step, various acid chlorides with different chain lengths (**4**, $-C_7H_{15}$; **5**, $-C_{13}H_{27}$; **6**, $-C_{17}H_{35}$) were attached. The products were recrystallized from methanol or THF. Because of the introduction of the long alkyl chain, the melting temperatures of these three derivatives and, concomitantly, their dissolution and crystallization temperatures in *i*-PP are much lower compared to those for compounds **1**−**3**. As expected, the melting temperatures decreased with increasing chain length: **4**; 225 °C; **5**, 215 °C; **6**, 211 °C. Compound **4**, with the shortest alkyl chain ($-C_7H_{15}$), has a dissolution

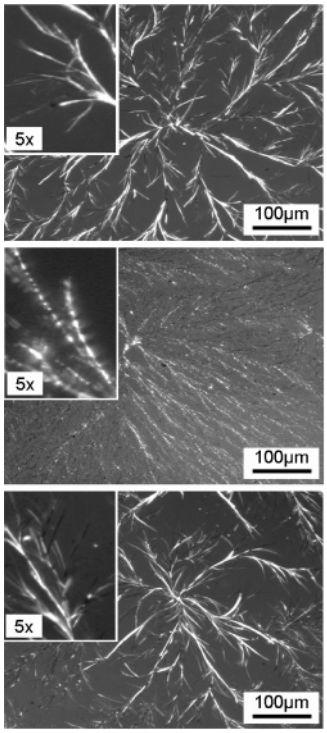

Figure 2. Optical micrographs featuring fine birefringent fibrillar structures of the three dicyclohexyl-substituted 1,4-phenylene−bisamide isomers **1** (top), **2** (middle) and **3** (bottom) (concentration 0.25 wt %) in the *i*-PP melt at 160 °C. The pictures were taken between crossed polarizers while cooling the sample from 260 °C after complete dissolution. The enlarged cutouts in the micrographs indicate that the asymmetric compound **2** forms twisted fibrillar branched aggregates upon crystallization, whereas the symmetric compounds form non-twisted branches.

temperature of 182 °C at a concentration of 0.25 wt % in the *i*-PP melt. The dissolution temperatures of compounds **5** and **6** could not be determined as no birefringent structures from the additives were observed at temperatures above the melting temperature of *i*-PP (165 °C). The crystallization temperatures decreased from 165 °C for compound **4** to 153 °C for compound **5** and 147 °C for compound **6** with increasing alkyl chain length. A similar formation of the three-dimensional dendritic structures as for compounds **1** and **3** was observed.

3.2. Nucleation of Isotactic Polypropylene. The nucleation ability of an additive depends on the epitaxial match between the growth planes of isotactic polypropylene and the specific surface of the additive. The latter strongly depends on the chemical structure of the molecules and their supramolecular arrangement. Within the discussed series, the influence of several structural variations on the crystallization behavior of i-PP can be revealed.

The first very decisive characteristic of a nucleated polymer, here *i*-PP, is its increased crystallization temperature (T_c) in comparison to the neat, unmodified material (T_c = 110 °C). Figure 3 top shows results for the crystallization temperature of *i*-PP/bisamide mixtures **1**−**3** as a function of the additive in the concentration range from 0.0005 to 0.25 wt %. Considering the structural similarity of these three dicyclohexyl-substituted bisamides **1**−**3**, one would expect a comparable nucleating efficiency. This is indeed the case as reflected by similar concentration dependence and comparable values for the crystallization temperature. For all three dicyclohexyl-substituted bisamides **1**−**3**, T_c was found to be only moderately altered at concentrations below 0.01 wt %, indicating that these molecules

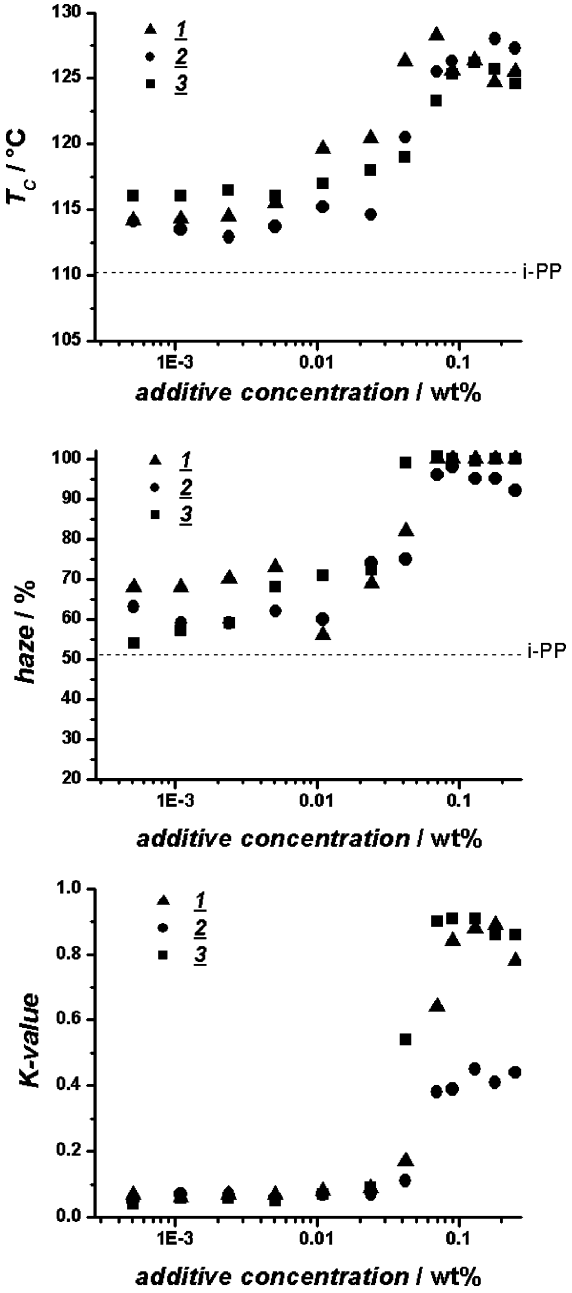

Figure 3. Dependence of the crystallization temperature (T_c) (top), haze (middle) and *k* value (bottom) of *i*-PP on the additive concentration of the dicyclohexyl-substituted 1,4-phenylene bisamides **1**−**3**. The haze values and *k* values were determined on injection molded *i*-PP plaques with 1.1 mm thickness.

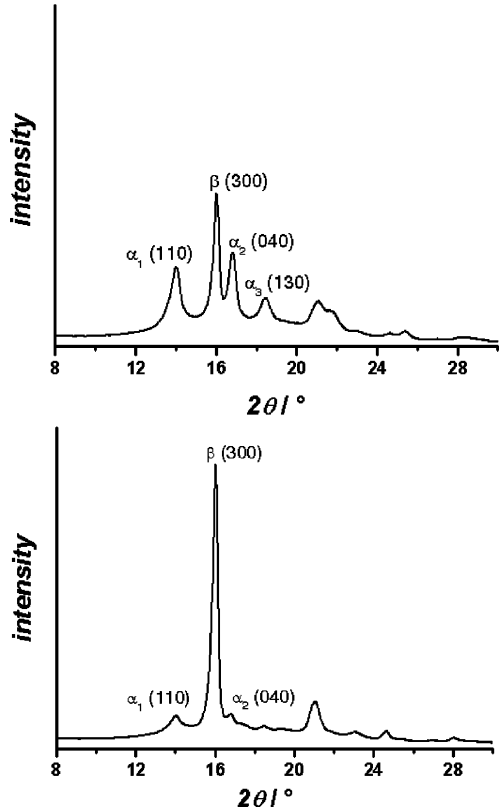

Figure 4. Wide-angle X-ray diffraction patterns of injection molded *i*-PP plaques (1.1 mm thickness) comprising the dicyclohexyl-substituted 1,4-phenylene bisamides **2** (top) and **3** (bottom) at a concentration of 0.13 wt %.

are not efficient nucleators at such low concentrations. A distinct increase in T_c was observed in the concentration range between 0.01 and 0.08 wt % followed by a saturation at $T_c = 125-128$ °C for concentrations in excess of 0.08 wt %.

It is well-known that symmetrical bisamides, such as *N*,*N*′-dicyclohexyl-2,6-naphthalenedicarboxamide (NU100) and *N*,*N*′-dicyclohexylterephthalamide (**1**), predominantly induce the β-polymorph of *i*-PP.[19−21,28−30] Isotactic polypropylene with a high β-content shows distinct property differences compared to α-*i*-PP. For example, injection molded specimens of β-*i*-PP are opaque which is reflected in high haze values close to 100%. Figure 3, middle, shows the additive concentration dependence of haze for injection-molded samples containing the dicyclohexyl-substituted bisamides **1**−**3**. As can be seen, they exhibit a haze value of ∼100% at concentration exceeding ∼0.08 wt %, which correlates very well with the increased crystallization temperature observed in the same concentration range. At lower additive concentrations, the haze decreases to values between 50% and 70%, closer to that of the reference material (51%), presumably due to the lower nucleation efficiency. Differences in haze may arise from either the presence of the β-crystal modification of *i*-PP or, alternatively, from scattering due to large additive aggregates. Therefore, wide-angle X-ray diffraction (WAXD) experiments were performed in order to determine the fraction of β-crystalline *i*-PP.[27] Two selected WAXD patterns are shown in Figure 4. The upper diagram displays the diffractogram for an injection-molded plaque (thickness 1.1 mm) of *i*-PP comprising 0.13 wt % of isomer **2** with asymmetrical orientation of the two amide groups. The most prominent signals of the α- and β-polymorphs of *i*-PP are indicated with their corresponding lattice planes, which for the α- modification are (110), (040), and (130) and for the β-modification is (300). From eq 1, a *k* value (β-content) of 0.45 was obtained for this sample. This modest *k* value revealed that compound **2**, being asymmetric with respect to the orientation of the amide groups, is not a highly efficient β-nucleating agent. On the contrary, at the same concentration (0.13 wt %), the symmetric compound **3** based on *p*-phenylendiamine clearly triggered formation of the β-phase as evidenced by a *k* value of this sample as high as 0.92 (cf. bottom WAXD diffractogram in Figure 4).

The concentration dependence of the *k* value for compounds **1**−**3** is shown in Figure 3, bottom. As can be clearly seen, the two symmetric compounds **1** and **3** induce very high β-contents ($k > 0.8$) at concentrations exceeding ∼0.08 wt %, whereas *k* values of only 0.35−0.45 were obtained for the symmetric bisamides at concentrations above 0.08 wt %. In all three cases,

in the concentration range where no nucleation occurred (<0.03 wt %), the *k* values are close to zero for all three compounds, and the samples predominantly crystallized in the common α-polymorph.

The surface morphology of crystals formed by compounds **1**−**3** contains cyclohexyl rings, which evidently provide a surface pattern for growth of *i*-PP. For compounds **1** and **3**, the arrangement of the cyclohexyl groups is expected to be symmetric with respect to the molecules, which most likely translates into highly symmetric aggregates formed upon recrystallization from the melt. For compound **2**, this cannot be the case in such perfection as the direction of one of the amide groups is inversed, and consequently, the symmetry of the molecule is lost. Interestingly, the crystallization temperatures were not changed by this structural variation. However, the *β*-content dramatically decreases for compound **2**, which may be explained by differences in the stacking behavior. Optical microscopy results provided strong evidence for helical self-assembly, which in view of the dissymmetry in the chemical structure seems feasible. The asymmetric orientation of the amide groups in compound **2** reduces the degree of freedom for formation of the hydrogen bonding pattern, which hampers the self-assembly process as reflected by the lower dissolution temperatures. In addition, a helical "hand" may be induced in the aggregates since the intermolecular hydrogen bonds can only be formed for one distinct way of packing. Thereby, aggregates with two slightly different surface patterns are expected to form, which we relate to the observed reduction of specificity for nucleating the *β*-polymorph of *i*-PP. In other words, although the cyclohexyl substituents seem favorable for nucleating the *β*-phase of *i*-PP, the crystallography of compound **2** must substantially differ from the two others.

The asymmetrically substituted bisamides **4**−**6** were also investigated in a similar manner, as shown in Figure 5. For all three derivatives, T_c is only slightly increased to temperatures around 115 °C throughout the entire concentration range. From these results, it may be concluded that the dicyclohexyl-substituted bisamides **1**−**3** are more efficient nucleating agents for *i*-PP than the asymmetrically substituted ones **4**−**6**. However, the observation of the influence of these derivatives on the haze of *i*-PP samples comprising these three derivatives with one long alkyl chain **4**−**6** shows an unexpected behavior (Figure 5 middle). The monoalkylated derivatives **5** ($-C_{13}H_{27}$) and **6** ($-C_{17}H_{35}$) increased the haze to ∼100% at concentrations in excess of 0.08 wt %, even though no changes in the crystallization temperature of *i*-PP had been observed in the investigated concentration range.

Interestingly, the mono-alkylated compounds **5** and **6** were also found to promote formation of the *β*-modification of *i*-PP to a certain extent, as evidenced from Figure 5 bottom. Although certainly not as efficient as compounds **1** and **3**, moderate *β*-contents were obtained: For additive concentrations of 0.1 wt % and more, compound **5** ($-C_{13}$ alkyl) induced a *β*-content (*k* value) of up to 0.7, whereas the sample containing compound **6** was characterized by a *k* value of ∼0.6. Thus, the high haze values observed in that same concentration range did indeed originate from the formation of the *β*-phase of *i*-PP and not from the presence of large additives aggregates, which could have been anticipated. Interestingly, compound **4** ($-C_7$ alkyl) seemingly did not trigger the predominant formation of the *β*-polymorph of *i*-PP.

In summary, the above results seem to indicate that for efficient *β*-nucleating agent (high *k* values), a high symmetry of the molecule and a layered sheetlike self-assembly are required. Helical self-assemblies promote rather the formation of α-modification, which may explain why no sorbitol-based *β*-nucleating agents have been found to date. The building blocks of this family of compounds induce helicity perse.[10,14]

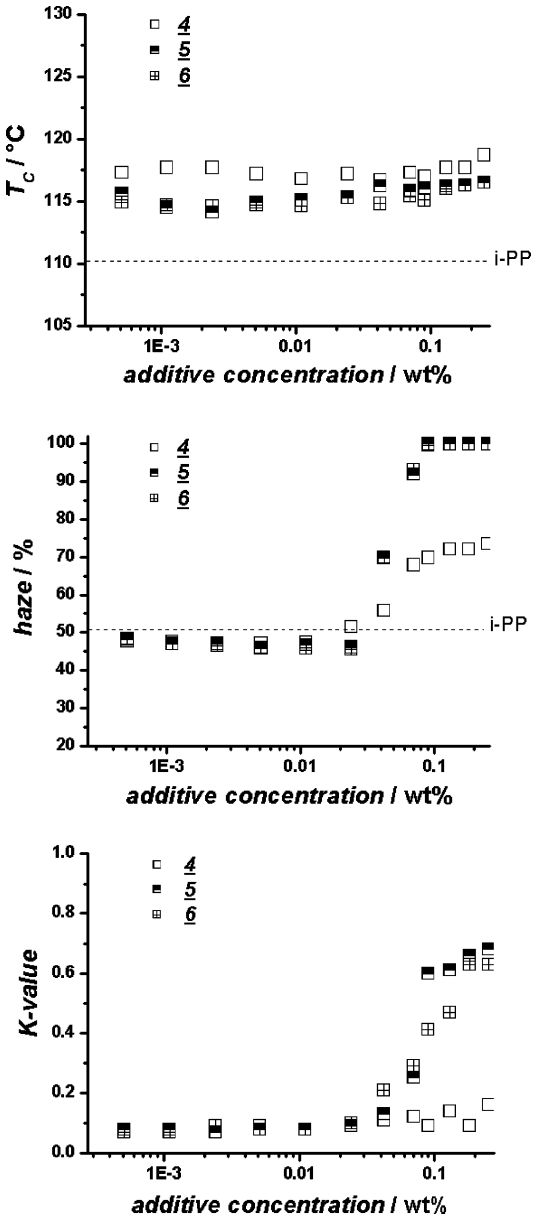

Figure 5. Dependence of the crystallization temperature (T_c) of *i*-PP (top), optical properties (haze) (middle) and of the *k* value (*β*-content) (bottom) on the additive concentration of the cyclohexyl/*n*-alkyl-substituted 1,4-phenylene bisamides **4**−**6**. The haze values and *k* values were determined on injection molded *i*-PP plaques with a thickness of 1.1 mm.

3.3. Electret Properties. In our previous work on triphenylamine-based electret additives for *i*-PP films, we concluded that for an efficient improvement of the charge storage properties the additives should be completely dissolved in the molten polymer during processing and upon cooling should self-assemble/crystallize into isolated nanostructures.[7] Otherwise a heterogeneous system with undissolved additive particles or a continuous ramified network structure is obtained. The latter could counteract the beneficial effect by providing pathways for charge drift and consequent neutralization.

The electret properties were determined as the surface potential of *i*-PP films, which were prepared from the injection-molded plaques by compression-molding between Kapton films

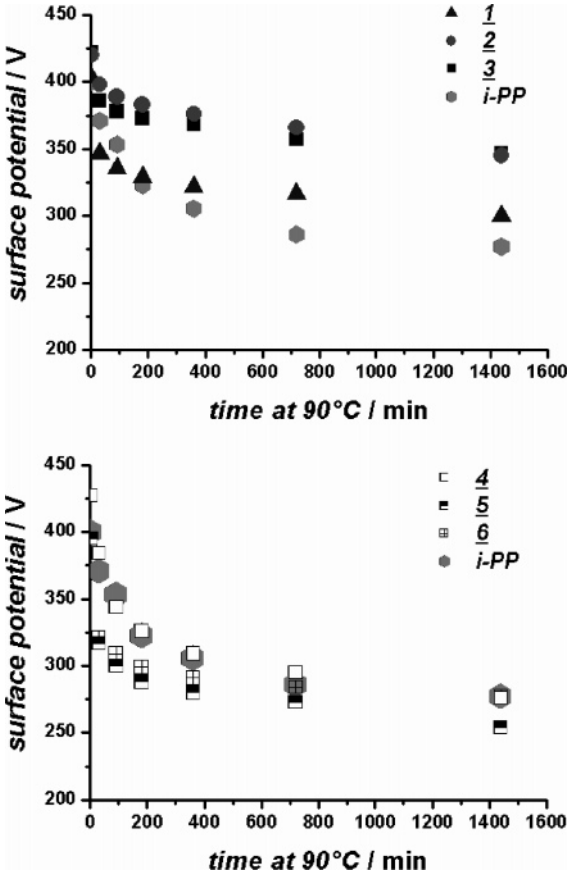

Figure 6. Surface potential as a function of annealing time at 90 °C for *i*-PP films comprising the dicyclohexyl-substituted 1,4-phenylene bisamides **1**−**3** (top) and the cyclohexyl/*n*-alkyl-substituted bisamides **4**−**6** at a concentration of 0.005 wt % (50 ppm) in comparison to the *i*-PP reference (solid hexagon). All films were initially charged employing a corona (tip-)voltage of +12.5 kV and a compensating grid set at a voltage of +400 V.

at 260 °C. Here, it should be noted that the surface of certain aromatic polyimides can induce trans-crystallization of polypropylene.[31] Sukhanova et al. investigated this phenomenon on polyimide fibers. However, for fibers of the same chemical structure as Kapton, no trans-crystallization was observed. The Kapton films used in this study showed only slight optical anisotropy and did also not induce trans-crystallization of *i*-PP, which was confirmed by optical polarized light microscopy of *i*-PP film cross sections prepared by regular microtomy.

The *i*-PP films with a thickness of 60 μm (5 cm × 5 cm) were charged with a corona setup resulting in initial surface potentials around 400 V. These films were subjected to accelerated aging at 90 °C for 1440 min (24 h) to simulate long-term behavior. During this time the surface potential was measured at room temperature after defined time periods. Figure 6 displays the decay of the surface potential as a function of annealing time at 90 °C for *i*-PP films containing 0.005 wt % of compounds **1**−**3** (top) and **4**−**6** (bottom) in comparison to the *i*-PP reference. The *i*-PP reference film exhibited a residual surface potential around 280 V after the annealing period of 24 h. Films comprising additives **2** and **3** display significantly higher charge storage capability, as indicated by a residual surface potential of 340 V after the same annealing time. Compound **1** improved only moderately (300 V) the surface potential in comparison to the reference material. In contrary, films with the more soluble additives **4**−**6** showed at concentration of 0.005 wt % surface potential values between 250 and

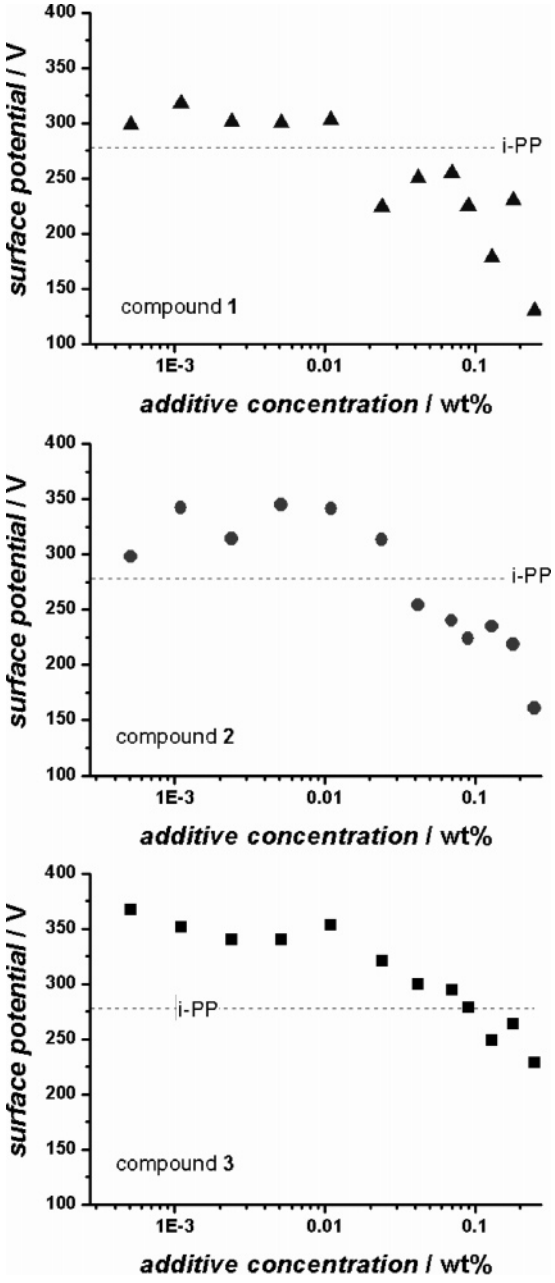

Figure 7. Additive concentration dependence of the surface potential (after accelerated aging at 90 °C for 24 h) of 50 μm thick *i*-PP films comprising the three different dicyclohexyl-substituted 1,4-phenylene bisamides **1**−**3**.

280 V. This is in the range of neat *i*-PP or even below. This observation indicates that these compounds **4**−**6** do not form isolated nanostructures, which can act as efficient charge traps.

To further elucidate the impact of the investigated bisamides on the charge storage behavior of *i*-PP, the residual surface potential (measured after 1440 min at 90 °C) was investigated as a function of additive concentration, results of which are presented in Figure 7 for compounds **1**−**3** and Figure 8 for compounds **4**−**6**, respectively. With all three isomers **1**−**3**, an improvement in the charge storage behavior was found at concentrations below the range from 0.02 to 0.06 wt %, almost independent of concentration. Above this concentration range, the residual surface potential dropped below the values of the reference for all three compounds. This behavior is in good agreement with the concentration dependence of the nucleation efficiency. At concentrations below this range, no mentionable

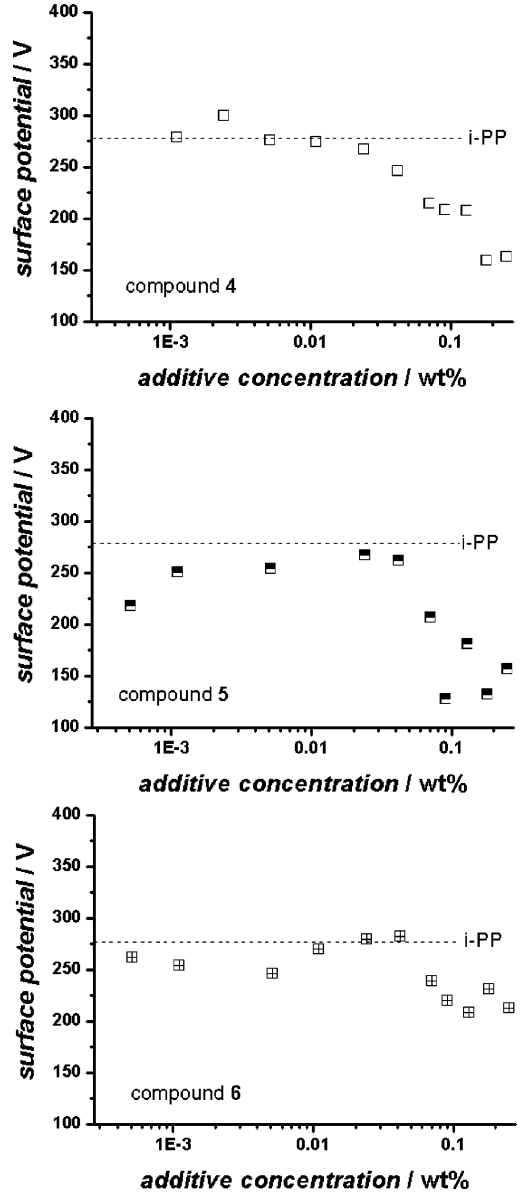

Figure 8. Additive concentration dependence of the surface potential (after accelerated aging at 90 °C for 24 h) of 50 μm thick *i*-PP films comprising the different cyclohexyl/*n*-alkyl-substituted bisamide **4**−**6**.

nucleation was observed, which we related to the formation of isolated, too-small nanoaggregates, not sufficient in number to nucleate *i*-PP throughout the entire bulk, but apparently sufficient to serve as charge traps. At concentrations exceeding this concentration range, the formation of a three-dimensional fibrillar network structure results in increasing nucleation efficiency but at the same time provides pathways for charge drift and neutralization, whereby the electret effect vanishes.

In contrast to the dicyclohexyl-substituted derivatives, the monoalkylated compounds **4**−**6** were not capable of improving the charge storage behavior of *i*-PP over the entire investigated concentration range as shown in Figure 8.

4. Conclusions

In the present study, we have demonstrated the importance of efficient β-nucleating agents for *i*-PP with high crystallization temperature and high *k* values having a highly symmetric molecular structure as is the case for the two dicyclohexyl-substituted 1,4-phenylene−bisamides **1** and **3**. Already the slightest deviation, inversion of one amide group, resulted in a decreased *k* value for compound **2**. With respect to the nucleation properties and the capability of improving the electret properties, two distinct concentration ranges were identified. For efficient nucleation, the additive concentration has to be above a critical concentration where a continuous network nanostructure of the nucleating agents is formed. However, this concentration regime was not suitable to improve the electret properties, because this percolating network provides pathways for the charges to drift and neutralization consequently occurred upon accelerated aging. At concentrations below the percolation threshold, isolated nanoaggregates are expected to form upon cooling, capable of acting as charge traps with concomitant loss in nucleation efficiency. Finally, introduction of *n*-alkyl chains seems to be, based on the investigated compounds, no way to efficient nucleating agents or electret additives.

Acknowledgment. We thank the Deutsche Forschungsgemeinschaft (DFG) for financial support (DFG-Projekt Schm 703/2-2; Al 474/5-2). We are grateful to Dr. Thomas Frese (Polymer Engineering, University Bayreuth) for setting up an electret laboratory. We are also indebted to Sandra Ganzleben and Jutta Failner (Macromolecular Chemistry I, University Bayreuth) for assistance in preparation of the polypropylene films. Many thanks go to Prof. Gerhard M. Sessler (Darmstadt University of Technology) for his continuous support on electrets and to Prof. Paul Smith (ETH Zürich) for the ongoing collaboration on nucleating agents and many fruitful discussions.

References and Notes

(1) Sessler, G. M. *Electrets*, 3rd ed.; Springer Verlag: New York, 1999; Vol. I.
(2) Kressmann, R.; Sessler, G. M. *IEEE Trans. Dielectr. Electr. Insul.* **1996**, *3*, 607.
(3) Guarrotxena, N.; Millan, J.; Sessler, G. M.; Hess, G. *Macromol. Rapid Commun.* **2000**, *21*, 691.
(4) Nath, R.; Perlman, M. M. *IEEE Trans. Dielectr. Electr. Insul.* **1989**, *24*, 409−412.
(5) Mittal, A.; Jain, V.; Mittal, J. *J. Mater. Sci. Lett.* **2001**, *20*, 681−685.
(6) Behrendt, N.; Mohmeyer, N.; Hillenbrand, J.; Klaiber, M.; Zhang, X.; Sessler, G. M.; Schmidt, H.-W.; Altstädt, V. *J. Appl. Polym. Sci.* **2006**, *99*, 650−658.
(7) Mohmeyer, N.; Müller, B.; Behrendt, N.; Hillenbrand, J.; Klaiber, M.; Zhang, X.; Smith, P.; Altstädt, V.; Sessler, G. M.; Schmidt, H.-W. *Polymer* **2004**, *45*, 6655−6663.
(8) Zweifel, H. *Plastics Additives Handbook*, 5th ed.; Hanser Verlag: Munich, 2001.
(9) Binsbergen, F. L. *Polymer* **1970**, *11*, 253.
(10) Kobayashi, T.; Hashimoto, T. *Bull. Chem. Soc. Jpn.* **2005**, *78*, 218−235.
(11) Hamada, K.; Uchiyama, H. US Patent 4,016,118.
(12) Mannion, M. J. US Patent 5,198,484.
(13) Marco, C.; Ellis, G.; Gomez, M. A.; Arribas, J. M. *J. Appl. Polym. Sci.* **2002**, *84*, 2440−2450.
(14) Kristiansen, M.; Werner, M.; Tervoort, T.; Smith, P.; Blomenhofer, M.; Schmidt, H.-W. *Macromolecules* **2003**, *36*, 5150−5156.
(15) Blomenhofer, M.; Ganzleben, S.; Hanft, D.; Schmidt, H.-W.; Kristiansen, M.; Smith, P.; Stoll, K.; Mäder, D.; Hoffmann, K. *Macromolecules* **2005**, *38*, 3688−3695.
(16) Marco, C.; Gomez, M. A.; Ellis, G.; Arribas, J. M. *J. Appl. Polym. Sci.* **2002**, *84*, 1669−1679.
(17) Yoshimoto, S.; Ueda, T.; Yamanaka, K.; Kawagushi, A.; Tobita, E.; Haruna, T. *Polymer* **2001**, *42*, 9627−9631.
(18) Menyhard, A.; Varga, J.; Molnar, G. *J. Therm. Anal. Calorimetry* **2006**, *83*, 625−630.
(19) Stocker, W.; Schumacher, M.; Graff, S.; Thierry, A.; Wittmann, J.-C.; Lotz, B. *Macromolecules* **1998**, *31*, 807−814.
(20) Mathieu, C.; Thierry, A.; Wittmann, I. C.; Lotz, B. *J. Polym. Sci., Part B: Polym. Phys.* **2002**, *40*, 2504−2515.
(21) Ikeda, N.; Yoshimura, M.; Mizoguchi, K.; Kawashima, Y.; Sadamitsu, K.; Wawahara, Y. EP 0557721 A2.
(22) Karger-Kocsis, J.; Varga, J.; Drummer, D. *J. Macromol. Sci. Phys.* **2002**, *B41*, 881−889.

(23) Raab, M.; Scudla, J.; Kolarik, J. *Eur. Polym. J.* **2004**, *40*, 1317−1323.
(24) Larocca, J. P.; Sharkawi, M. A. Y. *J. Pharm. Sci.* **1967**, *56*, 916−918.
(25) Mohmeyer, N.; Schmidt, H.-W. *Chem.—Eur. J.* **2005**, *11*, 863−872.
(26) ASTM Standard D 1003 Standard Test Method for Haze and Luminous Transmittance of Transparent Plastics. 1961.
(27) Turner-Jones, A.; Aizlewood, J. M.; Beckett, D. R. *Makromol. Chem.—Eur. J.* **1964**, *75*, 134.
(28) Varga, J.; Mudra, I.; Ehrenstein, G. W. *J. Appl. Polym. Sci.* **1999**, *74*, 2357.
(29) Varga, J. *J. Macromol. Sci. Polym. Phys.* **2002**, *41*, 1121.
(30) Chen, H. B.; Karger-Kocsis, J.; Wu, J. S.; Varga, J. *Polymer* **2002**, *43*, 6505.
(31) Sukhanova, T. E.; Lednicky, F.; Urban, J.; Baklagina, Y. G.; Mikhajlov, G. M.; Kudryavtsev, V. V. *J. Mater. Sci.* **1995**, *30*, 2201.

MA060340Q